Energetics of Nanoarchitectured TiO_2−ZrO_2 and TiO_2−MoO_3 Composite Materials

M. R. Ranade,† S. H. Elder,‡ and A. Navrotsky*,†

University of California at Davis, Thermochemistry Facility, Department of Chemical Engineering and Materials Science, Davis, California 95616, and Intel Corporation, Hillsboro, Oregon 97124

Received July 10, 2001. Revised Manuscript Received November 25, 2001

High-temperature drop solution calorimetry in sodium molybdate solvent was performed on nanoarchitectured materials using a Calvet twin microcalorimeter at 975 K. Nanocrystalline TiO_2−ZrO_2 samples (mesoporous structure) and nanocrystalline TiO_2−MoO_3 samples (core−shell structure) were investigated. With the use of the measured drop solution enthalpies, the transformation enthalpies to macroscopic stable crystalline phases have been calculated. The enthalpy of transformation from amorphous to monoclinic ZrO_2 obtained from this work, -50.08 ± 4.92 kJ/mol, is in reasonable agreement with the value of -58.60 ± 3.30 kJ/mol determined by Molodetsky et al. (2000). The enthalpy of transformation from amorphous to crystalline MoO_3 derived from these data is -51.25 ± 2.01 kJ/mol. The enthalpy of transformation of nanophase anatase to bulk macrocrystalline rutile TiO_2 is -7.02 ± 0.96 kJ/mol. The linear variation of energetics with the composition of both series, TiO_2−ZrO_2 and TiO_2−MoO_3, suggests that these materials constitute a nanoscopic two-phase mixture, with their energetics being a weighted sum of end-member enthalpies. The energetic effects of surface area and of phase transformations could not be separated because the surface area (m^2/mol) varies approximately linearly with mole fraction. Thermogravimetric analysis and differential thermal analysis corroborate the proposed energetic model. Thermodynamic stability issues of these nanoarchitectured materials are discussed along with structural aspects.

Introduction

Nanocrystalline materials play an important role in environment, agriculture, and technology.[1] Much research in nanomaterials has focused on semiconductor nanoparticles which display a variety of fundamentally interesting photophysical properties that are a direct result of their size and dimensionality.[2] The physical properties of nanocrystalline materials can be tailored to suit applications such as photoluminescence, solar energy conversion, and photocatalysis. Though nanocrystalline TiO_2 has been widely regarded as a potential material in photocatalytic applications,[3] it has a band gap of ∼3.2 eV, well outside the intense region of the solar spectrum centered at ∼2.6 eV. To make the band gap of TiO_2 suitable for practical solar energy conversion, nanoarchitectured materials with core−shell structure have been synthesized.[2]

TiO_2 can exist in several polymorphs (including anatase, brookite, and rutile) that can be crystallized at low temperatures in the laboratory and nature.[4−6] Although, under ambient conditions, macrocrystalline rutile is thermodynamically stable relative to anatase or brookite,[7,8] TiO_2 nanoparticles often exist as anatase and/or brookite. Upon being heated, the anatase and brookite modifications coarsen and convert to the thermodynamically stable rutile phase. Anatase nanoparticles were successfully grown in a mesoporous framework structure[9] that prevented their agglomeration, growth, and transformation to rutile.

In addition to controlling size and dimensionality, nanoarchitectured materials present the possibility of tailoring the physical properties (significantly different from the properties of their respective bulk materials) and may prove useful in important technological applications. The goal of this work is to understand the energetic stability of these nanoarchitectured materials by measuring thermochemical data. Such information is essential both for understanding fundamental solid-state chemistry and for predicting phase equilibria, compatibility of materials, and reactivity. Previously, using high-temperature oxide melt drop solution calorimetry for nanocrystalline Al_2O_3, it was shown that

* To whom correspondence should be addressed. E-mail: anavrotsky@ucdavis.edu.
† University of California at Davis.
‡ Intel Corporation.

(1) Navrotsky, A. *J. Nanopart. Res.* **2000**, *2*, 321.
(2) Elder, S. H.; Cot, F. M.; Su, Y.; Heald, S. M.; Tyryshkin, A. M.; Bowman, M. K.; Gao, Y.; Joly, A. G.; Balmer, M. L.; Kolwaite, A. C.; Magrini, K. A.; Blake, D. M. *J. Am. Chem. Soc.* **2000**, *122*, 5138.
(3) Fujishima, A.; Honda, K. *Nature* **1972**, *238*, 37.
(4) Bokhimi, Morales, A.; Novaro, O.; Lopez, T.; Sanchez, E.; Gomez, R. *J. Mater. Res.* **1995**, *10*, 2788.
(5) Ye, X. S.; Sha, J.; Jiao, Z. K.; Zhang, L. D. *Nanostruct. Mater.* **1997**, *8*, 919.
(6) Banfield, J. F.; Bischoff, B. L.; Anderson, M. A. *Chem. Geol.* **1993**, *110*, 211.
(7) Zhang, H.; Banfield J. F. *J. Mater. Chem.* **1998**, *8*, 2073.
(8) Navrotsky, A.; Kleppa, O. J. *J. Am. Ceram. Soc.* **1967**, *50*, 626.
(9) Elder, S. H.; Gao, Y.; Li, X.; Liu, J.; McCready, D. E.; Windisch, C. F. *Chem. Mater.* **1998**, *10*, 3140.

10.1021/cm010607u CCC: $22.00
Published on Web 01/29/2002

γ-Al_2O_3 (the phase observed for nanosized particles) is more stable in enthalpy than nanophase α-Al_2O_3 (where α (corundum) is the macrocrystalline thermodynamically stable phase).[10,11] Such a phase stability reversal at the nanoscale has been predicted for nanocrystalline TiO_2.[7,10] Energetics of nanoarchitectured materials can provide insight into the thermal stability issues essential for rational and efficient processing of materials to realize the full potential of these nanomaterials.

Experimental Section

Synthesis. To synthesize TiO_2-ZrO_2 composites, $(NH_4)_2Ti(OH)_2(C_3H_5O_3)_2$ (Tyzor LA from DuPont, 2.23 M in Ti), $(NH_4)_2Zr(OH)_2(CO_3)_2$ (AZC from Magnesium Electron Inc., 14.8 wt % Zr), and cetyltrimethylammonium chloride (CTAC, 29 wt % from Lonza Chemical Co. Inc.) were combined in appropriate molar ratios. The resulting clear mixture was stirred while slowly adding water. A white precipitate was immediately formed, which readily dissolved upon stirring. Precipitate formation and dissolution continued until the original mixture was diluted by a factor of 5, at which point irreversible precipitation occurred. The irreversible precipitation continued until the original mixture was diluted by a factor of 10. The white precipitate was stirred overnight at room temperature and aged for 60 h at 373 K first and then overnight at 423 K in a sealed Teflon reactor. The product was then washed and centrifuged several times with water and dried at 313 K for 24 h. The powder was calcined at 623 K for 2 h to remove CTAC. The resultant solid was a free flowing white powder. All the syntheses were performed in a similar fashion to obtain the entire $(1 - x)TiO_2-xZrO_2$ series.

To synthesize TiO_2-MoO_3 composites, $(NH_4)_2Ti(OH)_2(C_3H_5O_3)_2$ (Tyzor LA from DuPont, 2.23 M in Ti), $Na_4Mo_8O_{26}$, and CTAC (29 wt % from Lonza Chemical Co. Inc.) were combined in appropriate molar ratios. Vigorous stirring of the solution resulted in a voluminous white precipitate. The mixture was stirred at room temperature overnight, at 343 K for 24 h, and at 373 K for 48 h in a sealed Teflon reactor. The precipitate was washed and centrifuged several times with water. CTAC was removed by calcining in air at 623 K for 2 h. All the syntheses were performed similarly to obtain the $(1 - x)TiO_2$-$xMoO_3$ solid solution series. It was possible to synthesize TiO_2-MoO_3 samples within the range $x = 0.03$ to 0.3, but above $x > 0.3$, the synthesis attempts resulted in bulk TiO_2 and MoO_3, indicating a macroscopic phase separation. [2]

Pure anatase was synthesized from a mixture of $(NH_4)_2Ti(OH)_2(C_3H_5O_3)_2$ (Tyzor LA from DuPont, 2.23 M in Ti) and CTAC (29 wt % from Lonza Chemical Co. Inc.). A white precipitate was formed when water was added. Vigorous stirring readily dissolved the white precipitate. The addition of water and stirring were continued until irreversible precipitation occurred. The reaction was stirred first at room temperature overnight, then at 343 K for 24 h, and finally at 373 K for 48 h in a sealed Teflon reactor. The precipitate was washed and centrifuged several times with water. The sample was calcined at 623 K for 2 h in air to remove CTAC.

TiO_2 rutile, Alfa Aesar (Puratronic 99.995% metals basis, Stock no. 10897, Lot no. 21826), and MoO_3, Alfa Aesar (Puratronic, 99.9995% metals basis, Stock no. 12930, Lot no. 22429), were used in calorimetry to complete the thermochemical cycles. Rutile and MoO_3 were heated at 973 and 673 K, respectively, overnight for removal of moisture. The heat-treated samples were used for calorimetry.

The moisture sensitive nanocrystalline samples were handled in a glovebox filled with inert Ar gas (oxygen < 1 ppm and moisture < 1 ppm). In addition to being moisture sensitive, TiO_2-MoO_3 composites are light sensitive. These samples were wrapped in aluminum foil to prevent light exposure inside the glovebox.

Characterization. The sample characterization using X-ray diffraction (XRD), elemental analyses, Brunauer−Emmett−Teller (BET) technique, transmission electron microscopy (TEM), Raman spectroscopy, and electron paramagnetic resonance (EPR) has been reported previously.[2,9] In this study, the samples were further characterized by thermogravimetric analysis and differential thermal analysis (TG/DTA) and measurement of water content. The TG/DTA was performed using a Netzsch STA 409. Water contents of the samples were determined using weight loss measurements. TiO_2-ZrO_2 and TiO_2-MoO_3 samples, accurately weighed inside a glovebox, were heated for 12 h at 1473 and 973 K, respectively, to remove water. The difference between the final weight and the initial weight is assumed to be the amount of water in the sample. The molar compositions (formula weights) were normalized to obtain 1 mole of sample and y moles of water. Table 1 reports the composition of the samples (based on water corrections coupled with the elemental analyses) and specific surface area (BET) for TiO_2-ZrO_2 and TiO_2-MoO_3 series.

Calorimetry. High-temperature drop solution calorimetry in $3Na_2O{\cdot}4MoO_3$ solvent was performed in a custom-built Tian-Calvet twin microcalorimeter described in detail by Navrotsky.[12,13] Oxygen gas was flushed through the glassware above the solvent at ~90 mL/min and bubbled through the calorimetric solvent at ~5 mL/min. The samples were pressed in the form of pellets (~15 mg) inside the glovebox, weighed, and stored in a glass vial. When a stable baseline (signal from the thermopiles of the calorimeter) was obtained, then the pellet from the glass vial was dropped into the calorimeter. The total time for which the pellet was exposed to the atmosphere was 5−10 s. In the case of the light sensitive TiO_2-MoO_3 samples, after weighing, the pellets were transferred to the small side chamber of the glovebox to prevent light exposure. The total light exposure of the sample, while pressing the pellet and dropping into the calorimeter, was less than 5 min. The calorimetric conditions were identical for the drop solution experiments of nanocrystalline anatase and the reference compounds, namely, commercial Alfa Aesar TiO_2 (rutile) and MoO_3 (molybdite). The calibration was performed using corundum pellets of similar weight.

Results and Discussion

Sample Description. TiO_2-ZrO_2 nanocomposites possess a framework structure. These mesoporous materials are structured about a surfactant-templated, disordered porous network with a uniform pore diameter of about 2.5 nm.[9] The anatase TiO_2 phase is preserved in this nanocomposite due to the surrounding ZrO_2 that prevents coarsening and phase transformation. In this surfactant directed inorganic framework, the diameter of the pores in the network dictates the maximum particle size of anatase. The BET surface areas expressed in m^2/mol vs the mole fraction of ZrO_2 show an approximately linear trend (Figure 1a). The individual contribution of TiO_2 and ZrO_2 to the surface area cannot be separated and may be complex because of the nanostructured morphology (as is also the case for the TiO_2-MoO_3 system). The roughly linear variation of surface area (m^2/mol) with mole fraction suggests that, to a first approximation, the surface area of the composite can be described as that of a mechanical mixture of anatase of surface area 12 000 m^2/mol (150 m^2/g) and amorphous zirconia of surface area 42 000 m^2/mol (341 m^2/g). This approximation will be used later

(10) McHale, J. M.; Auroux, A.; Perrota, A. J.; Navrotsky, A. *Science* **1997**, *277*, 788.
(11) McHale, J. M.; Navrotsky, A.; Perrota, A. J. *J. Phys. Chem.* **1997**, *101*, 603.
(12) Navrotsky, A. *Phys. Chem. Miner.* **1997**, *24*, 222.
(13) Navrotsky, A. *Phys. Chem. Miner.* **1977**, *2*, 89.

Table 1. Thermochemical Data (Drop Solution Enthalpies and Transformation Enthalpies) and Surface Area for TiO_2-ZrO_2 and TiO_2-MoO_3 Nanocomposites

				ΔH_{ds} (kJ/mol)[a]		
sample	composition	surface area by BET (m^2/g)	surface area by BET (m^2/mol)	without water corrn	with water corrn	ΔH_{trans} (kJ/mol) measured
57001−151	pure anatase TiO_2, 0.027 H_2O	150	11984.7	52.79 ± 0.65 (8)	50.93 ± 0.65 (8)	−7.02 ± 0.96
SHE00120A	0.1 ZrO_2, 0.9 TiO_2, 0.26 H_2O	140	11792.2	55.65 ± 0.60 (6)	37.71 ± 0.60 (6)	−16.41 ± 2.02
SHE00120B	0.25 ZrO_2, 0.75 TiO_2, 0.22 H_2O	150	13608.0	37.64 ± 0.65 (6)	22.46 ± 0.65 (6)	−25.93 ± 2.04
SHE00125	0.48 ZrO_2, 0.52 TiO_2, 0.37 H_2O	350	35241.5	35.86 ± 0.48 (7)	10.33 ± 0.48 (7)	−29.26 ± 1.99
SHE00121B	0.75 ZrO_2, 0.25 TiO_2, 0.36 H_2O	270	30345.3	19.18 ± 0.45 (7)	−5.66 ± 0.45 (7)	−34.92 ± 1.98
ZrO_2	pure monoclinic ZrO_2				19.7 ± 1.8 (7)[b]	−58.60 ± 3.30 [c]
rutile	Alfa Aesar Puratronic TiO_2				57.95 ± 0.71 (23)	
MoO_3	Alfa Aesar Puratronic				72.85 ± 0.61 (7)	−48.91 ± 4.2 [d]
SHE00116A	0.03 MoO_3, 0.97 TiO_2, 0.04286 H_2O	125	10237.5	53.15 ± 0.64 (7)	50.19 ± 0.64 (7)	−8.21 ± 0.94
SHE00116B	0.1 MoO_3, 0.9 TiO_2, 0.1683 H_2O	200	17280.0	56.25 ± 0.81 (8)	44.64 ± 0.81 (8)	−14.81 ± 1.14
SHE00116C	0.25MoO_3, 0.75 TiO_2, 0.2817 H_2O	205	19680.0	62.73 ± 1.06 (8)	43.29 ± 1.06 (8)	−18.38 ± 1.20
SHE00116D	0.3 MoO_3, 0.7 TiO_2, 0.2253 H_2O	150	14865.0	59.04 ± 0.96 (9)	43.49 ± 0.96 (9)	−18.94 ± 1.10

[a] Value is the mean of the number of experiments indicated in the parentheses. Error is the two standard deviations of the mean. [b] Molodetsky et al. (2000).[24] [c] Enthalpy of amorphization of ZrO_2 from Molodetsky et al. (2000).[14] [d] Enthalpy of fusion of MoO_3 at 1074 K from JANAF.[16]

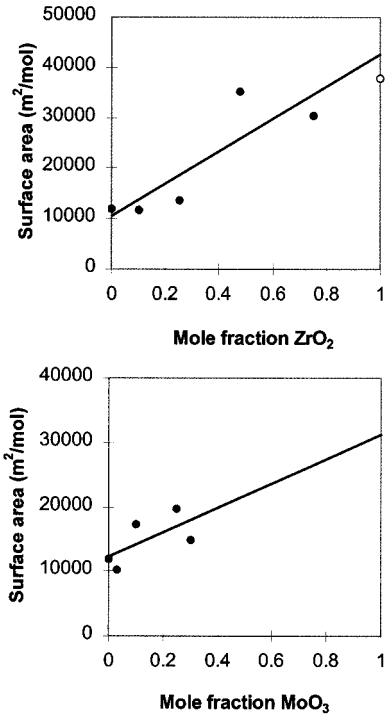

Figure 1. Surface area vs mole fraction: (a) TiO_2-ZrO_2 nanocomposites. The solid symbols represent the values obtained in this work. The open symbol shows the calculated surface area based on the average TEM diameter of amorphous ZrO_2 from a previous study of differently prepared amorphous ZrO_2[14] and (b) TiO_2-MoO_3 nanocomposites.

in discussion of the thermochemistry. More details of structure and characterization of the TiO_2-ZrO_2 nanocomposites are provided elsewhere.[9]

The TiO_2-MoO_3 nanocomposites possess a core−shell structure with an anatase core surrounded by a MoO_3 shell. With increase in mole fraction of MoO_3 in the nanocomposite, the shell evolves from less than a monolayer to two monolayers. This structural geometry prevents the agglomeration, growth, and transformation of the anatase TiO_2 core. The surface area (m^2/mol) of the sample varies approximately linearly with the mole fraction of MoO_3 (Figure 1b). The surface area can be represented as a linear combination of that of anatase of surface area 12 000 m^2/mol (150 m^2/g) and amorphous MoO_3 of surface area 30 000 m^2/mol (208 m^2/g). A detailed description of TiO_2-MoO_3 nanocomposites is provided elsewhere.[2]

Thermochemical Analysis. One goal of this study is to compare the measured enthalpies of the nanostructured TiO_2-ZrO_2 and TiO_2-MoO_3 composites to the enthalpy of a mechanical mixture of well-crystallized macroscopic samples of TiO_2 (rutile), ZrO_2 (baddeleyite), and MoO_3 (molybdite). The latter represent the stable polymorphs at 298 K. Differences in the energetics of the nanocomposite and a mechanical mixture of the same composition may arise from several factors: polymorphism in ZrO_2, MoO_3, and TiO_2, surface energy terms in the nanophase materials, any chemical interactions between TiO_2 and ZrO_2 or TiO_2 and MoO_3 in the nanocomposite, and the presence of adsorbed water.

Because there is no evidence for strong chemisorption of H_2O on TiO_2, ZrO_2, or MoO_3 (all H_2O is lost in TG/DTA scans below 500 K), we correct for the presence of water using a thermochemical cycle (see C1−C3 in Appendix), which assumes that the H_2O present has the enthalpy of bulk liquid water. Loosely bound/physisorbed water has been observed in our previous studies of amorphous ZrO_2 and nanocrystalline TiO_2.[14,15] The enthalpy of reaction of the samples with water

(14) Molodetsky, I.; Navrotsky, A.; Paskowitz, M. J.; Leppert, V. J.; Risbud, S. H. *J. Non-Cryst. Solids* **2000**, *262*, 106.

$$TiO_2\,(\text{nano, 298 K}) + 0.027H_2O\,(\text{liq, 298 K}) \rightarrow TiO_2{\cdot}0.027H_2O\,(\text{nano, 298 K}) \quad (1)$$

$$xZrO_2{\cdot}(1-x)TiO_2\,(\text{nano, 298 K}) + yH_2O\,(\text{liq, 298 K}) \rightarrow xZrO_2{\cdot}(1-x)TiO_2{\cdot}yH_2O\,(\text{nano, 298 K}) \quad (2)$$

$$xMoO_3{\cdot}(1-x)TiO_2\,(\text{nano, 298 K}) + yH_2O\,(\text{liq, 298 K}) \rightarrow xMoO_3{\cdot}(1-x)TiO_2{\cdot}yH_2O\,(\text{nano, 298 K}) \quad (3)$$

is assumed to be negligible. The drop solution enthalpies with and without water corrections are listed in Table 1. The correction for H_2O can be quite substantial, reaching nearly 50% of the total heat effect in some samples (Table 1). The water-corrected drop solution enthalpies for TiO_2-ZrO_2 and TiO_2-MoO_3 nanocomposites are plotted against the mole fractions of ZrO_2 or MoO_3 in Figures 2a and 2b. The drop solution data, for both composite series, are also constrained using the drop solution enthalpy of pure anatase (Table 1). The solid straight lines are least-squares fits to the data (solid symbols). Figure 2 also shows, as open symbols and a dashed line, the drop solution enthalpy of a mechanical mixture of macroscopic TiO_2 (rutile), ZrO_2 (baddeleyite), and MoO_3 (molybdite). The drop solution enthalpies for both series vary approximately linearly with the mole fraction (Figures 2a 2b). This linear variation suggests that the enthalpy of each system behaves like that of a mechanical mixture of nanostructured end-members. The XRD data suggest that these nano end-members are TiO_2 anatase, amorphous ZrO_2, and amorphous MoO_3. The enthalpy of each of these should depend on its surface area. However, as Figure 1 shows, the measured surface area depends approximately linearly on the mole fraction. Therefore the enthalpic effects of surface area and of composition cannot be separated. Rather, the nano end-members can be taken to be TiO_2 anatase with a surface area of about 12 000 m^2/mol, amorphous ZrO_2 with a surface area of about 42 000 m^2/mol, and amorphous MoO_3 with a surface area of about 30 000 m^2/mol.

Thermochemical cycles (refer to C2 and C3) are used to determine the transformation. The measured transformation enthalpies are given in Table 1. The transformation enthalpies refer to the following reactions at 298 K

$$xZrO_2{\cdot}(1-x)TiO_2\,(\text{nanocomposite}) = xZrO_2\,(\text{baddeleyite}) + (1-x)TiO_2\,(\text{rutile}) \quad (4)$$

or

$$xMoO_3{\cdot}(1-x)TiO_2\,(\text{nanocomposite}) = xMoO_3\,(\text{molybdite}) + (1-x)TiO_2\,(\text{rutile}) \quad (5)$$

where the baddeleyite, molybdite, and rutile are coarse grained while the starting nanoarchitectured composites have their as-synthesized small particle size. A general expression for the transformation enthalpy for the

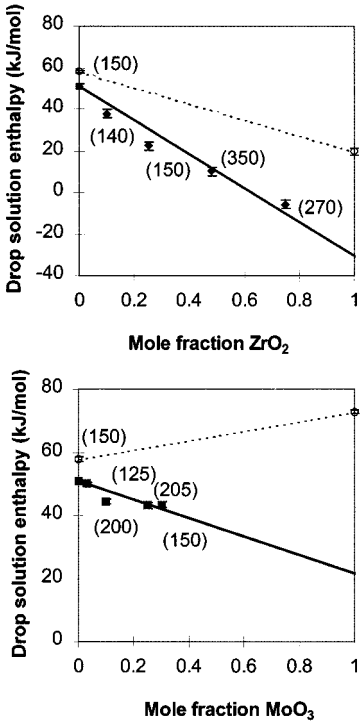

Figure 2. Drop solution enthalpies vs mole fraction, after corrections for H_2O content, for (a) TiO_2-ZrO_2 nanocomposites and (b) TiO_2-MoO_3 nanocomposites. The data are shown as solid symbols, and the solid line represents the nanocomposite samples. The open symbols and the dashed line joining them represents the enthalpy of a macroscopic mixture of bulk crystalline phases. The difference between a point on the dashed line and the solid symbols represents the enthalpy of transformation (ΔH_{trans}) from nanocomposite to bulk material (see Table 1 and Discussion in text). Numbers in parentheses represent the surface area (m^2/g) of the sample.

nanocomposites can be written as

$$\Delta H_{trans} = x(\Delta H_{trans,A}) + (1-x)(\Delta H_{trans,B}) + x(\text{area}_A\gamma_A) + (1-x)(\text{area}_B\gamma_B) + x(1-x)W(x) \quad (6)$$

where A represents TiO_2 and B represents either ZrO_2 or MoO_3, γ is the surface energy, and $W(x)$, a composition-dependent interaction function, corresponds to the enthalpy of any interaction between TiO_2 and ZrO_2 or TiO_2 and MoO_3.

As discussed above, the effect of surface area on energetics cannot be separated from the enthalpy of transformation. However, the data suggest that the enthalpy of interaction, $W(x)$, between TiO_2 and ZrO_2 or TiO_2 and MoO_3 in the nanocomposite is small ($W <$ 10 kJ/mol in magnitude), since no systematic deviation from linearity, as would be expected for an interaction function, is seen within the uncertainty of our measurements. A simplified version of reaction 6 can be written as

$$\Delta H_{trans} = x(\Delta H_{trans,A} + \text{area}_A\gamma_A) + (1-x)(\Delta H_{trans,B} + \text{area}_B\gamma_B) = xC_1 + (1-x)C_2 \quad (7)$$

where the constant (C) terms include both transformation and surface enthalpy terms.

(15) Ranade, M. R.; Navrotsky, A.; Zhang, H. Z.; Banfield, J. F.; Elder, S. H.; Borse, P. H.; Kulkarni, S. K.; Doran, G. S.; Whitfield, H. J. *Proc. Natl. Acad. Sci.*, in press.

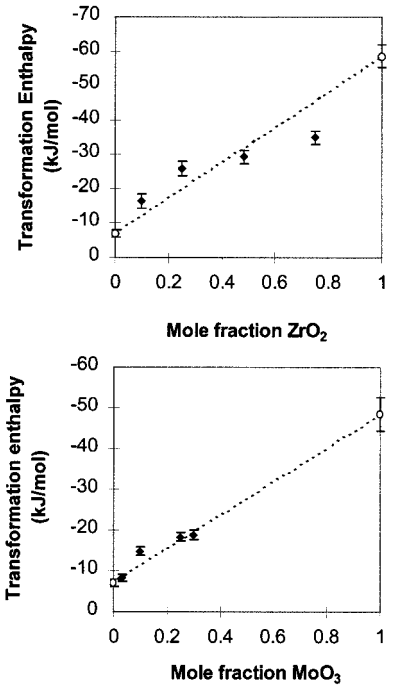

Figure 3. Transformation enthalpies to bulk crystalline phases vs mole fraction for (a) TiO_2−ZrO_2 composites and (b) TiO_2−MoO_3 composites. The solid diamond symbol represents the measured transformation enthalpies, and the open symbols and the dashed line joining them represents a mechanical mixture of transformation enthalpies of the nano end-members (see Discussion in text).

Reactions (4) and (5) can then be written as

$$x\mathrm{ZrO_2}\cdot(\text{amorphous, 42 000 m}^2/\text{mol}) + (1-x)\mathrm{TiO_2}\,(\text{anatase, 12 000 m}^2/\text{mol}) = x\mathrm{ZrO_2}\,(\text{baddeleyite}) + (1-x)\mathrm{TiO_2}\,(\text{rutile}) \quad (8)$$

$$x\mathrm{MoO_3}\cdot(\text{amorphous, 30 000 m}^2/\text{mol}) + (1-x)\mathrm{TiO_2}\,(\text{anatase, 12 000 m}^2/\text{mol}) = x\mathrm{MoO_3}\,(\text{molybdite}) + (1-x)\mathrm{TiO_2}\,(\text{rutile}) \quad (9)$$

The TEM results for amorphous ZrO_2 from the previous study indicate the average diameter of particles to be 3.5 nm,[14] which translates into a calculated surface area, 37 720 m^2/mol, which is very close to the value obtained here (see Figure 1a).

We may compare these measured transformation enthalpies to ones calculated using independent data for the end-members. The measured transformation enthalpies for TiO_2−ZrO_2 and for TiO_2−MoO_3 are represented graphically as Figures 3a and 3b. The dashed straight line in Figure 3a is drawn between the enthalpy of transformation from anatase to rutile (this work, Table 1) and the enthalpy of transformation from amorphous to monoclinic ZrO_2 measured on a low-temperature preparation of amorphous ZrO_2.[14] For the TiO_2−MoO_3 series, the enthalpy of transformation of amorphous to crystalline MoO_3 is unknown. However, the enthalpy of fusion of MoO_3 is 48.53 ± 4.2 kJ/mol (JANAF).[16] JANAF takes the glass transition temperature to be 750 K, without justification. That value is different from other reported values that range from 623[17] to 643−673 K.[18] The enthalpy of vitrification at 298 K, calculated from JANAF data, by extrapolating the liquid heat capacity to 750 K and assuming the heat capacity of MoO_3 glass to be equal to the heat capacity of the crystal, is 41.44 ± 4.2 kJ/mol. Despite the uncertainties in assigning the glass transitions, we anticipate that the enthalpy of vitrification lies close to the range of values listed in JANAF[16] (from 48.53 ± 4.2 to 41.44 ± 4.2 kJ/mol). Therefore, we have used the enthalpy of crystallization of MoO_3, −48.53 ± 4.2 kJ/mol, from JANAF[16] as an estimate of the enthalpy of transformation of amorphous MoO_3 to molybdite. This estimate does not include an explicit surface energy term.

To verify the transformation enthalpy of the amorphous to the macrocrystalline stable monoclinic form of ZrO_2, we have used the following approach. The extrapolation of drop solution enthalpies for TiO_2−ZrO_2 nanocomposites (Figure 2a) to pure ZrO_2 yields the enthalpy of drop solution of amorphous ZrO_2 as −30.38 ± 4.58 kJ/mol. With the use of this drop solution enthalpy for amorphous ZrO_2, the enthalpy of transformation from amorphous to monoclinic ZrO_2 (refer to thermochemical cycle C4) is −50.08 ± 4.92 kJ/mol, slightly less exothermic than −58.60 ± 3.30 kJ/mol which was measured previously.[14] Although the TiO_2−ZrO_2 composites from this study have somewhat different surface areas with respect to each other and with respect to the amorphous sample used previously,[14] the extrapolation of the drop solution enthalpies yields a transformation enthalpy similar to the value obtained previously.

Although some researchers reported synthesis of amorphous MoO_3 as bulk[17−19] or as thin films,[20,21] they did not characterize the amorphous MoO_3 to establish structural or thermodynamic data. In this study, we used the TiO_2−MoO_3 samples from this study to derive the thermodynamic data. The MoO_3 shells on the TiO_2 cores in the TiO_2−MoO_3 series of compounds exist in an amorphous form.[2] The extrapolation of the drop solution enthalpies of TiO_2−MoO_3 nanocomposites (Figure 2b) yields the drop solution enthalpy of amorphous MoO_3 as 21.60 ± 1.92 kJ/mol. With the use of this value, the enthalpy of transformation of amorphous to crystalline MoO_3 (molybdite) is −51.25 ± 2.01 kJ/mol (refer to thermochemical cycle C5), in good agreement with the enthalpy of fusion listed by JANAF.[16] To our knowledge, this is the first experimental measurement of enthalpy of transformation from amorphous to crystalline MoO_3. We realize that these extrapolations are long, but the data seem reasonable and other samples could not be made at the time of this work due to difficulties in synthesis. Clearly, more work needs to be done in the synthesis and subsequent characterization of the amorphous MoO_3 compound.

(16) Chase, M. W., Jr. *NIST-JANAF Thermochemical Tables, J. Phys. Chem. Reference Data*; Monograph No 9; New York, 1998.

(17) Dong, W.; Dunn, B. *J. Non-Cryst. Solids* **1998**, *225*, 135.

(18) Mendez-Viviar, J.; Campero, A.; Livage, J.; Sanchez, C. *J. Non-Cryst. Solids* **1990**, *121*, 26.

(19) Yanovskaya, M. I.; Obvintseva, I. E.; Kessler, V. G.; Galyamov, B. Sh.; Kucheiko, S. I.; Shifrina, R. R.; Turova, N. Ya. *J. Non-Cryst. Solids* **1990**, *124*, 155.

(20) Yang, Y. A.; Cao, Y. W.; Loo, B. H.; Yao, J. N. *J. Phys. Chem. B* **1998**, *102*, 9392.

(21) Maruyama, T.; Kanagawa, T. *J. Electrochem. Soc.* **1995**, *142* (5), 1644.

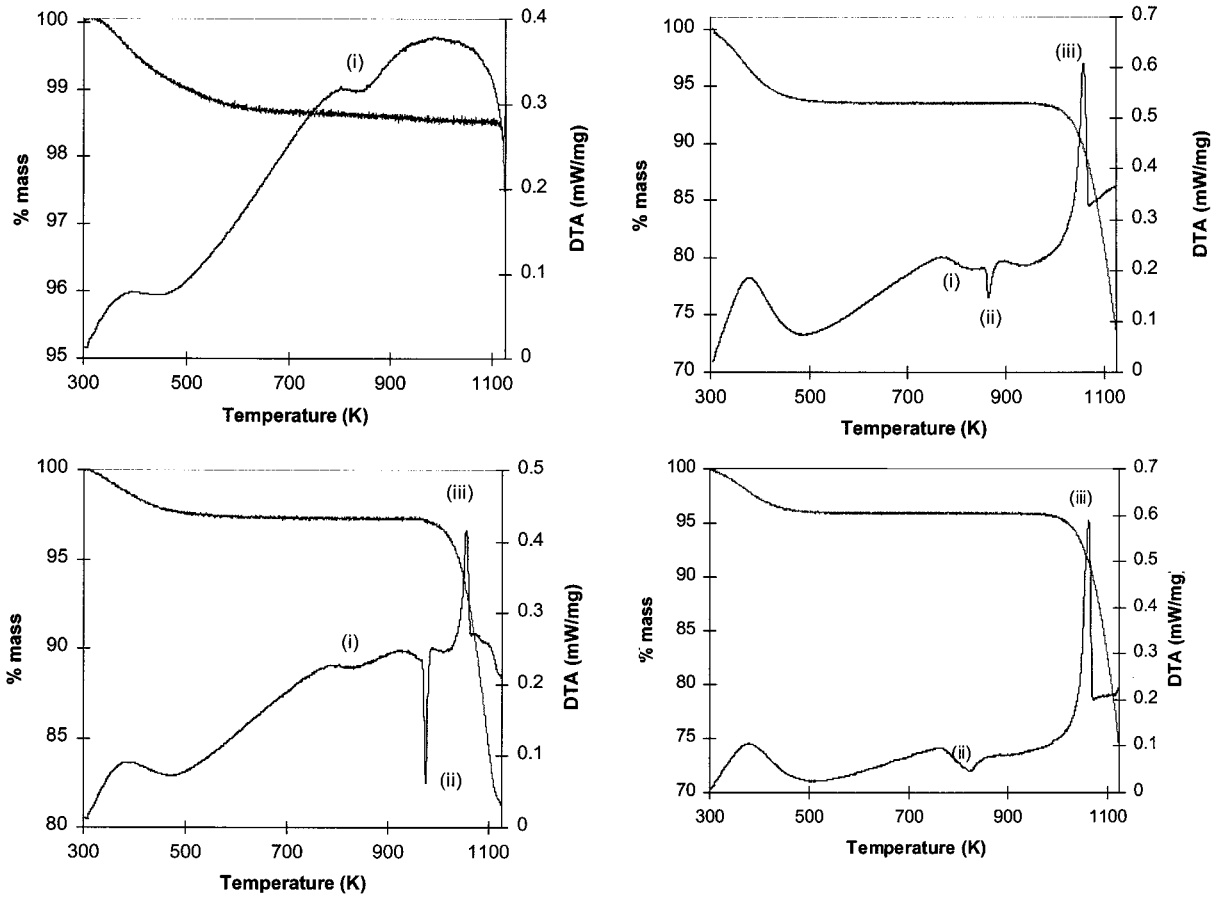

Figure 4. Thermal analysis (TG/DTA scans) of TiO_2-MoO_3 composites for (a) SHE00116A, (b) SHE00116B, (c) SHE00116C, and (d) SHE00116D.

Table C1. Thermochemical Cycle To Calculate the Transformation Enthalpy for Pure Anatase

$TiO_2 \cdot 0.027H_2O$ (nano, 298 K) → TiO_2 (soln, 975 K) + $0.027H_2O$ (g, 975 K)	ΔH_1
$0.027H_2O$ (g, 975 K) → $0.027H_2O$ (l, 298 K)	ΔH_2
TiO_2 (nano, 298 K) + 0.027 H_2O (l, 298 K) → $TiO_2 \cdot 0.027$ H_2O (nano, 298 K)	ΔH_3
TiO_2 (soln, 975 K) → TiO_2 (rutile, 298 K)	ΔH_4
TiO_2 (nano, 298 K) → TiO_2 (rutile, 298 K)	ΔH_5

$\Delta H_5 = \Delta H_1 + \Delta H_2 + \Delta H_3 + \Delta H_4$
$= 52.79\ (0.65) + 0.027^* (-69) - 57.946\ (0.706)$
$= 50.927 - 57.946$
$= -7.019\ (0.96)$ kJ/mol

It is interesting that this simple approach using end-member data appears to be a good first approximation. The complex morphology of the nanocomposites makes it hard to say whether the BET surface area measurements truly capture the surface areas of both components. The estimation of enthalpy of amorphous MoO_3 relative to bulk MoO_3 from the heat of fusion data works, perhaps, surprisingly well. The data for nanophase anatase have been discussed in more detail in a separate paper,[15] in which the transformation enthalpies and surface enthalpies of the TiO_2 (rutile−anatase−brookite) system are presented. What is encouraging in this first study of the energetics of nanocomposites is that a rather simple approach appears to capture the main features of the energetic behavior.

This simple thermochemical behavior in turn suggests that the complex nanoarchitecture is kinetically controlled by the synthesis conditions and templating agent(s) and that, other than the effect of polymorphism and surface area, any specific energy terms associated with the nano−meso-scale architecture are small and can probably be neglected.

Structural Evolution of TiO_2-MoO_3 Nanocomposites (TG/DTA). We studied $x MoO_3 \cdot (1 - x)TiO_2$ nanocomposites (where $x = 0.03-0.3$ for samples SHE00116A−D) using TG/DTA (Parts a−d of Figure 4). The water loss, observed in TG, is in good agreement with weight loss experiments. The first endothermic peak in the DTA curves for all samples (Parts a−d of Figure 4) is due to water loss. An exothermic peak at ~825 K marked as (i) corresponds to the crystal growth of the TiO_2 (anatase) core particles. A conversion of anatase phase to the rutile modification would have been an exothermic effect, similar to peak (i). However, this possibility was ruled out by XRD data that showed absence of any peaks corresponding to rutile phase. An exothermic peak (marked as (ii) in parts b−d of Figure 4) represents the crystallization of MoO_3, as confirmed by XRD data of the sample, before and after the transition temperature. As the amount of MoO_3 in the

Table C2. Thermochemical Cycle To Calculate the Transformation Enthalpy for TiO_2−ZrO_2 Compounds

$x$$ZrO_2$·$(1-x)$$TiO_2$·$y$$H_2O$ (nano, 298 K) → $x$$ZrO_2$ (soln, 975 K) + $(1-x)$$TiO_2$ (soln, 975 K) + $y$$H_2O$ (gas, 975 K)	ΔH_6
$y$$H_2O$ (gas, 975 K) → $y$$H_2O$ (l, 298 K)	ΔH_7
$x$$ZrO_2$·$(1-x)$$TiO_2$ (nano, 298 K) + $y$$H_2O$ (l, 298 K) → $x$$ZrO_2$·$(1-x)$$TiO_2$·$y$$H_2O$ (nano, 298 K)	ΔH_8
$(1-x)$$TiO_2$ (soln, 975 K) → $(1-x)$$TiO_2$ (rutile, 298 K)	ΔH_9
$x$$ZrO_2$ (soln, 975 K) → $x$$ZrO_2$ (monoclinic, 298 K)	ΔH_{10}
$x$$ZrO_2$·$(1-x)$$TiO_2$ (nano, 298 K) → $x$$ZrO_2$ (monoclinic, 298 K) + $(1-x)$$TiO_2$ (rutile, 298 K)	ΔH_{11}

$\Delta H_{11} = \Delta H_6 + \Delta H_7 + \Delta H_8 + \Delta H_9 + \Delta H_{10}$

SHE00120A
$= 55.65(0.60) + 0.26(-69) + 0.9 * (-57.95)(0.71) + 0.1 * (-19.7)(1.8)$
$= 37.71 - 52.15 - 1.97$
$= -16.41 \pm 2.02$ kJ/mol

SHE00120B
$= 37.64(0.65) + 0.22(-69) + 0.75 * (-57.95)(0.71) + 0.25 * (-19.7)(1.8)$
$= 22.46 - 43.46 - 4.93$
$= -25.93 \pm 2.04$ kJ/mol

SHE00125
$= 35.86(0.48) + 0.37(-69) + 0.52 * (-57.95)(0.71) + 0.48 * (-19.7)(1.8)$
$= 10.33 - 30.13 - 9.46$
$= -29.26 \pm 1.99$ kJ/mol

SHE00121B
$= 19.18(0.45) + 0.36(-69) + 0.25 * (-57.95)(0.71) + 0.75 * (-19.7)(1.8)$
$= -5.66 - 14.49 - 14.77$
$= -34.92 \pm 1.98$ kJ/mol

Table C3. Thermochemical Cycle To Calculate the Transformation Enthalpy for TiO_2−MoO_3 Compounds

$x$$MoO_3$·$(1-x)$$TiO_2$·$y$$H_2O$ (nano, 298 K) → $x$$MoO_3$ (soln, 975 K) + $(1-x)$$TiO_2$ (soln, 975 K) + $y$$H_2O$ (gas, 975 K)	ΔH_{12}
$y$$H_2O$ (gas, 975 K) → $y$$H_2O$ (l, 298 K)	ΔH_{13}
$x$$MoO_3$·$(1-x)$$TiO_2$ (nano, 298 K) + $y$$H_2O$ (l, 298 K) → $x$$MoO_3$·$(1-x)$$TiO_2$·$y$$H_2O$ (nano, 298 K)	ΔH_{14}
$(1-x)$$TiO_2$ (soln, 975 K) → $(1-x)$$TiO_2$ (rutile, 298 K)	ΔH_{15}
$x$$MoO_3$ (soln, 975 K) → $x$$MoO_3$ (molybdite, 298 K)	ΔH_{16}
$x$$MoO_3$·$(1-x)$$TiO_2$ (nano, 298 K) → $x$$MoO_3$ (molybdite, 298 K) + $(1-x)$$TiO_2$ (rutile, 298 K)	ΔH_{17}

$\Delta H_{17} = \Delta H_{12} + \Delta H_{13} + \Delta H_{14} + \Delta H_{15} + \Delta H_{16}$

SHE00116A
$= 53.15(0.64) + 0.04286(-69) + 0.97 * (-57.95)(0.71) + 0.03 * (-72.85)(0.61)$
$= 50.19 - 56.21 - 2.19$
$= -8.21 \pm 0.94$ kJ/mol

SHE00116B
$= 56.25(0.81) + 0.1683(-69) + 0.9 * (-57.95)(0.71) + 0.1 * (-72.85)(0.61)$
$= 44.64 - 52.16 - 7.29$
$= -14.81 \pm 1.14$ kJ/mol

SHE00116C
$= 62.73(1.06) + 0.2817(-69) + 0.75 * (-57.95)(0.71) + 0.25 * (-72.85)(0.61)$
$= 43.29 - 43.46 - 18.21$
$= -18.38 \pm 1.20$ kJ/mol

SHE00116D
$= 59.04(0.96) + 0.2253(-69) + 0.7 * (-57.95)(0.71) + 0.3 * (-72.85)(0.61)$
$= 43.49 - 40.57 - 21.86$
$= -18.94 \pm 1.10$ kJ/mol

Table C4. Thermochemical Cycle To Calculate the Transformation Enthalpy for Amorphous to Monoclinic ZrO_2

ZrO_2 (monoclinic, 298 K) → ZrO_2 (soln, 975 K)	ΔH_{18}
ZrO_2 (amorphous, 298 K) → ZrO_2 (soln, 975 K)	ΔH_{19}
ZrO_2 (amorphous, 298 K) → ZrO_2 (monoclinic, 298 K)	ΔH_{20}

$\Delta H_{20} = \Delta H_{19} - \Delta H_{18}$

Table C5. Thermochemical Cycle To Calculate the Transformation Enthalpy for Amorphous to Molybdite MoO_3

MoO_3 (molybdite, 298 K) → MoO_3 (soln, 975 K)	ΔH_{21}
MoO_3 (amorphous, 298 K) → MoO_3 (soln, 975 K)	ΔH_{22}
MoO_3 (amorphous, 298 K) → MoO_3 (molybdite, 298 K)	ΔH_{23}

$\Delta H_{23} = \Delta H_{22} - \Delta H_{21}$

TiO_2−MoO_3 series increases ($x = 0.1$−0.3 for samples SHE00116B−D), the crystallization temperature decreases from 975 to 825 K. The sample $0.03MoO_3$·$0.97TiO_2$, having the smallest amount of MoO_3, does not show peak (ii). For $0.3MoO_3$·$0.7TiO_2$ (SHE00116D), with the highest MoO_3 contents, the anatase (TiO_2 core) crystal growth coincides with the MoO_3 crystallization (at ~825 K) thus making it difficult to separate these two effects. The endothermic peak (marked as (iii) in parts b−d of Figure 4) occurs due to the melting of MoO_3 at 1058 K. Peak (iii) in DTA is accompanied by a weight loss in TG that may be due to reduction of MoO_3 to MoO_2, loss of MoO_3 (which possesses a high vapor pressure), or both. The reduction reaction should make the sample blue/black, which was not observed for these samples, and hence that possibility was ruled out. We did not investigate the loss of MoO_3 to avoid contamination due to condensation of MoO_3 on other parts of the instrument. The results from TG/DTA are consistent with the previously proposed structural model for TiO_2−MoO_3 core−shell materials,[2] and they provide an insight into the structural evolution of this nanoarchitectured material.

Implications of Energetics to Other Nanoarchitectured Materials. In addition to providing a guideline to study the energetics of similar nanoarchitectured materials (e.g., core−shell systems reported in the literature [22,23]), these results may be applicable to a

more general scenario. The core−shell TiO_2−MoO_3 material can be viewed as a coating of one material (amorphous MoO_3) on another (anatase TiO_2), in some ways analogous to a thin film grown on a substrate or analogous to native oxide growth in some elemental materials (e.g., Al_2O_3 film on Al metal or SiO_2 film on Si wafer). The interpretation of the energetics of these materials may indeed be similar to that of the TiO_2−MoO_3 nanocomposites. Currently, we are developing a calorimetric methodology to determine energetics of oxide and nitride thin films. We anticipate that the data interpretation for thin film calorimetry may be similar to that of nanoarchitectured composites. Such interpretations might constitute the basis for understanding the energetics of more complicated materials, namely, quantum dots, quantum wells, and laser superstructures in semiconductors.

Nanoparticles of iron and aluminum oxides and oxyhydroxides transport both organic and inorganic contaminants in the environment. The systematics developed here may be applied to understanding such natural nanocomposites. For example, it may be possible to treat coatings of amorphous uranium or chromium oxides on nanophase (Fe, Al)OOH particles as a mixture of nanophase end-members from the point of view of energetics.

Conclusions

The energetics of both nanoarchitectured materials, namely, TiO_2−ZrO_2, with mesoporous framework structures, and TiO_2−MoO_3, with core−shell structures suggest that these materials constitute a nanoscopic mechanical mixture of the respective nanophase end-members. A linear correlation between the surface area and the molar composition prevents us from separating the effects of the surface energy and phase transformations. The enthalpy of transformation for amorphous (∼42 000 m^2/mol) to coarse-grained monoclinic ZrO_2 is −50.08 ± 4.92 kJ/mol, in reasonable agreement with the previously determined transformation enthalpy, −58.60 ± 3.30 kJ/mol,[14] measured for an amorphous sample prepared by low-temperature synthesis, which has a surface area of ∼37 720 m^2/mol. The enthalpy of transformation from amorphous to crystalline MoO_3 is −51.25 ± 2.01 kJ/mol.

Acknowledgment. The National Science Foundation(Grants EAR 9725020 and 0123998) supported the work of A.N. and M.R.R. at UC Davis. A portion of this work was performed at the William R. Wiley Environmental Molecular Sciences Laboratory, a national user facility, at Pacific Northwest National Laboratory, which is operated by Battelle for the U. S. Department of Energy. S.H.E. is grateful to the Office of Basic Energy Sciences, Division of Materials Science, for supporting this work.

Appendix: Thermochemical Cycles

See Tables C1−C5.

CM010607U

(22) Yang, C. S.; Liu, Q.; Kauzlarich, S. M. *Chem. Mater.* **2000**, *12*, 983.

(23) Plaza, R. C.; Zurita, L.; Duran, D. G.; Gonzalez-Caballero, F.; Delgado, A. V. *Langmuir* **1998**, *14*, 6850.

(24) Molodetsky, I.; Navrotsky; A.; DiSalvo, F. J.; Lerch, M. *J. Mater. Res.* **2000**, *15* (11), 2558.